

# Solution-Processed Infrared Optoelectronics: Photovoltaics, Sensors, and Sources

Edward (Ted) H. Sargent, *Senior Member, IEEE*

(Invited Paper)

**Abstract**—The fabrication of optoelectronic devices via spin-coating onto an arbitrary substrate offers ease of integration, low cost, and physical flexibility. Reports of active optoelectronic devices operating in the IR, and made via solution-processing, emerged in the early 2000s. Here, we review progress in IR solar cells, image sensors, and optical sources based on solution-processed materials. The latest solution-processed photovoltaics (PV) now provide 4.2% power conversion efficiencies in the IR, placing them a factor of 3 away from enabling a doubling in overall solar power conversion efficiency of today's best visible-wavelength solution-processed PV. The best solution-processed photodetectors now provide sensitivities in the  $10^{13}$  Jones  $D^*$  range, exceeding the sensitivity of the best epitaxially grown short-wavelength infrared photodetectors. Infrared optical sources, both broadband light-emitting diodes and, more recently, lasers, have now also been reported at 1.5  $\mu\text{m}$ . We review the progress and future prospects of this rapidly advancing field.

**Index Terms**—Electroluminescence, modulation, photodetectors, photovoltaic cells, quantum confined Stark effect, quantum dots.

## I. INTRODUCTION

### A. Need for Solution-Processed Optoelectronics

**H**IGHLY perfected crystalline semiconductors are at the heart of the information age. An astonishing and still-growing density of silicon-based integration powers computing. Terabit-per-second fiber-optic communication depends on semiconductor lasers, modulators, and photodetectors that generate, manipulate, and sense light with efficiency and speed.

Many emerging clean energy technologies are also underpinned by pure, perfect crystalline semiconductors. Crystalline silicon-based solar cells can convert 25% of the sun's energy reaching the earth into electrical power [1]. When even higher efficiencies are needed, multijunction solar cells consisting of a stacked series of visible and infrared photovoltaic devices reach 32% power conversion efficiency.

As an example, creating silicon characterized by purity and crystalline perfection generally requires crystal growth at temperatures well above 1000 °C. Since crystals of a given composition have a defined lattice constant, combining multiple materials on a single substrate necessitates either finding crys-

tal pairings that are lattice-matched or near-matched, or finding ways to tolerate or buffer mismatch [2].

The successful integration, atop a single substrate, of a number of different semiconductor materials, each possessing a different bandgap, is of crucial importance to a significant number of applications (Fig. 2). In energy conversion, multijunction cells provide the only means of achieving the upper reaches of power conversion efficiency in view of the sun's broad spectrum. In communications and computing, silicon dominates purely electronic operations, whereas compound semiconductors such as InP, GaAs, and their alloys facilitate optoelectronic operations. The monolithic integration of optical communications and electronic computing on a chip is a long-sought goal in long-haul fiber-optic communication and intrachip communication alike [3].

As a consequence, there is an urgent need for high-performance optoelectronic materials strategies compatible with an arbitrary substrate. In the ideal, to achieve a maximum of versatility, such materials would:

- 1) enable *high-performance* devices that, at a minimum, meet the requirements of the application they are to address; or, better yet, compete with or even outstrip their conventional epitaxial counterparts;
- 2) be highly *tunable*, enabling convenient modification of their spectral properties, such as their bandgap and absorption/emission spectra, within a single materials system;
- 3) be conveniently *integrable*, relying on simple methods such as solution-processing (e.g., spin-casting or spray-coating, as is done dozens of times per wafer in integrated circuit engineering) to cover large areas of substrate;
- 4) be *physically flexible*, enabling roll-to-roll processing of large, low-cost devices such as solar panels, and offering integrability with fabrics for wearability;
- 5) be manufacturable at *low cost* per device area.

While all of these features are generally desired, their relative importance varies from application to application. In monolithic integration of optoelectronic devices on a silicon electronics platform, high performance, tunability, and integrability are paramount; whereas physical flexibility may play some role in facilitating packaging, and low cost per device area is usually more than satisfied compared to other system components. In contrast, in solar energy conversion, low cost, integrability, and physical flexibility are paramount in making environmentally sustainable technologies economically inevitable; and bandgap tunability is absolutely essential to enable multijunction

Manuscript received January 24, 2008; revised May 6, 2008.

E. H. Sargent is with the Department of Electrical and Computer Engineering, University of Toronto, Toronto, ON M5S 3G4, Canada (e-mail: ted.sargent@utoronto.ca).

Color versions of one or more of the figures in this paper are available online at <http://ieeexplore.org>.

Digital Object Identifier 10.1109/JSTQE.2008.925766

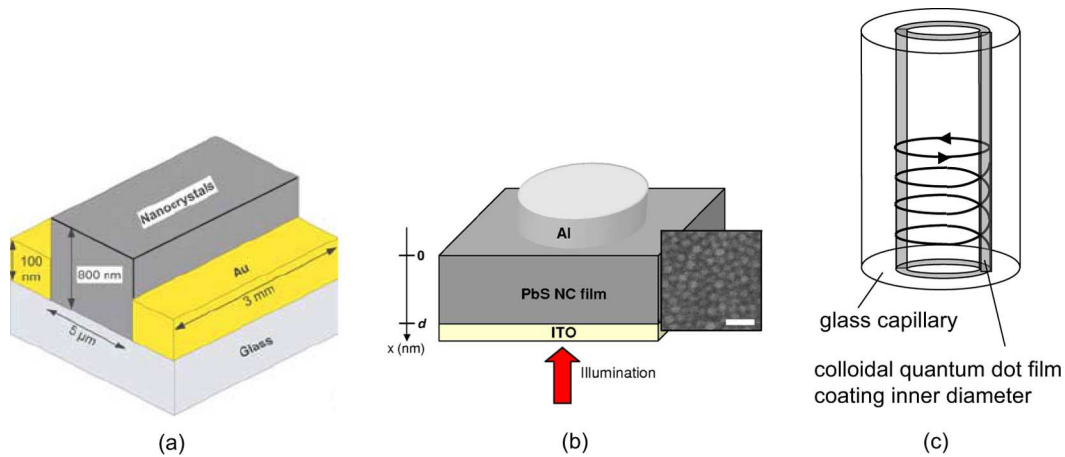


Fig. 1. Device geometries in which (a) photodetectors (b) solar cells and (c) lasers have been demonstrated based on infrared solution-processed colloidal quantum dots. (a) Lateral photoconductive photodetector. (b) Vertical infrared (IR) solar cell. (c) Whispering gallery mode laser with quantum dot active region.

architectures—it is a prerequisite for high power conversion efficiencies.

Solution-processing opens a variety of methods for the formation of the active region of a semiconductor device. Among the simplest optoelectronic devices to fabricate are those illustrated in Fig. 1(a), in which all needed electrical contacts are already disposed on the substrate prior to active layer fabrication, and thus, the active medium can simple be spin-cast or spray-coated from a solvent (typically organic) atop the electrodes. Vertical device geometries such as the photovoltaic device of Fig. 1(b) also employ simple solution-processing, but require overlayers such as a top contact that may be applied using vacuum techniques, or increasingly, using compatible solution-processing technologies for electrical contacts. An interesting variant on these methods is the device of Fig. 1(c) in which the active layer of a laser has been deposited inside a capillary simply via dip-coating followed by drying.

A key research question underlies this field: can application-relevant performance be achieved within low-cost, large-area solution-processed materials strategies? Put another way, are purity, crystalline perfect, and high-temperature processing requirements for semiconductor device performance?

### B. Infrared Optoelectronics

The above-mentioned features of a desirable optoelectronic-device-enabling class of materials make no mention of wavelength, other than noting the desirability of tunability. In fact, wavelength is of principal concern in applications in imaging, photovoltaic power conversion, and on-chip optical source provision.

In each case, interaction with visible light is of central interest, and has been widely explored. With good reason, sensing of visible colors underpins the vast majority of contemporary digital imaging applications [4]. As for PV, half of the sun's power lies in the visible spectral band, and thus, much effort in both conventional [1] and solution-processed [5] solar cells has been devoted to harvesting within the visible spectral regime. Efficient optical power generation in the visible region is central to lighting and displays, and here, once again, large-area low-cost solutions are urgently needed and are also advancing rapidly [6].

In the present review, we focus instead on the IR spectral region (Fig. 2).

The reasons for interest in this spectral regime are, once again, application-dependent. We next discuss the particular infrared bands of interest in PV, imaging, and communications.

With respect to PV, the sun's distribution of spectral power (Fig. 2) across the visible, near-infrared (NIR), and short-wavelength infrared (SWIR) mandates that if a solar cell is to be made from a single junction, the bandgap of the light-absorbing medium is best chosen to lie at  $1.1 \mu\text{m}$ , at the beginning of the SWIR. Even if two junctions (a tandem solar cell) or three junctions are employed, all of the constituent materials are optimally chosen to have bandgaps in the near or short-wave infrared.

In the field of imaging, the troposphere's nightglow provides continuous illumination of all outdoor scenes [7], but with over 90% of the illuminating power residing between 1200 and 1800 nm. Passive night vision is therefore possible using image sensors capable of seeing across the SWIR.

Finally, in communications, fiber optics relies on spectral bands lying within the range  $1.3\text{--}1.6 \mu\text{m}$  [8] in view of glass optical fiber's low absorption and dispersion within certain bands in this range. For on-chip optical communication, signal routing in transparent waveguides integrated on silicon is most readily achieved if wavelengths not absorbed by silicon, thus lying beyond  $1.1 \mu\text{m}$ , are employed [3].

In sum, there exists tremendous applied impetus to realize the advantages of solution-processed optoelectronics within the IR.

## II. PHOTOVOLTAICS (PV)

### A. Bandgap Requirements for Efficient PV

As seen in Fig. 2, the sun's spectrum spans the visible, the NIR, and a major portion of the SWIR. Indeed half the sun's power lies in the IR beyond 700 nm.

If a solar cell is to be made using a single semiconductor junction, and if we assume that all photons more energetic than the light-absorbing semiconductor's bandgap are substantially absorbed and harvested, while those lying below the bandgap remain unabsorbed, then simple analysis of the sun's power spectrum reaching the earth leads to an optimal choice of

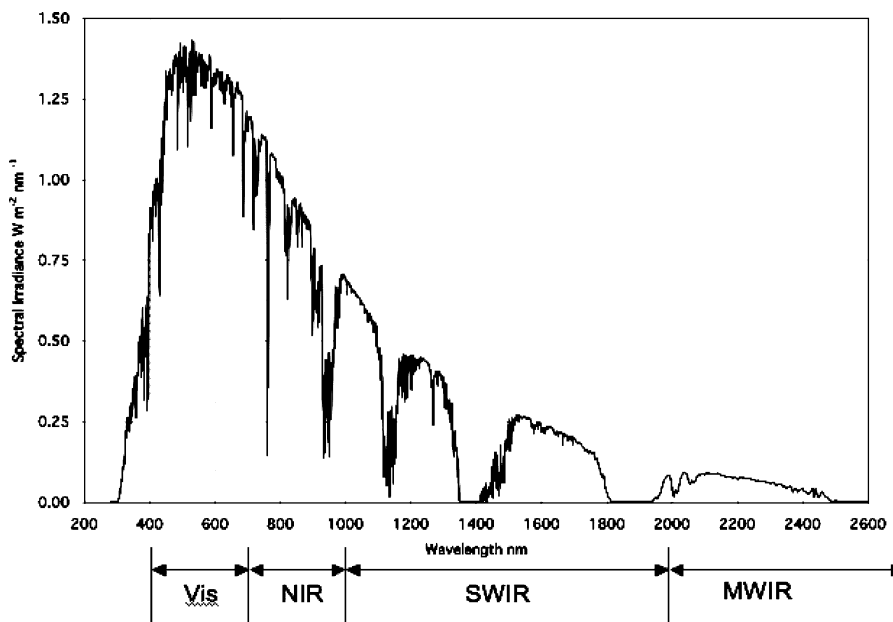


Fig. 2. Sun's spectrum reaching the earth (AM1.5). The portions residing in the visible (Vis), near infrared (NIR), SWIR, and mid-wavelength infrared (MWIR) are shown.

TABLE I  
MAXIMUM EFFICIENCIES, AND OPTIMAL CHOICES OF BANDGAP (SINGLE-JUNCTION)/BANDGAPS (MULTIJUNCTION), IN THE CASE OF UNCONCENTRATED AND CONCENTRATOR-BASED SOLAR CELLS CALCULATION IS BASED ON THE AM1.5 SOLAR SPECTRUM. TAKEN FROM [35]

Number of junctions	If unconcentrated (1 sun)		If maximally concentrated:	
	Limiting efficiency	Optimal bandgap(s)	Limiting efficiency	Optimal bandgap(s)
1	32.5	1.13 eV 1.10 $\mu\text{m}$	44.6	0.94 eV 1.32 $\mu\text{m}$
2	44.1	0.94, 1.64 eV 1.32, 0.76 $\mu\text{m}$	59.4	0.71, 1.41 eV 1.75, 0.88 $\mu\text{m}$
3	49.7	0.71, 1.16, 1.83 eV 1.75, 1.07, 0.68 $\mu\text{m}$	66.6	0.69, 1.16, 1.84 eV 1.80, 1.07, 0.67 $\mu\text{m}$

bandgap. While further decrease of the bandgap beyond this optimum would increase the fraction of the sun's power absorbed, it would also lower the open-circuit voltage of the device. For unconcentrated rays (1 sun), the optimal bandgap of such a single-junction cell is 1.13 eV, corresponding to a wavelength of 1.1  $\mu\text{m}$  (Table I). Silicon, with its 1.11 eV bandgap, is an excellent choice from this standpoint, though, since direct transitions only become possible in silicon above about 3 eV, its absorption is relatively weak throughout much of the visible and all of silicon's IR-absorbing region. This entails the need for a large thickness of material if light is to be substantially absorbed—and thus, large silicon thickness is a requirement if this material is to achieve high external quantum efficiency and thus power conversion efficiency.

In sum, the optimal single-junction solar cell has its bandgap in the SWIR. In spite of this fact, the vast majority of solution-processed solar cell work employs materials that absorb principally in the visible. The reason for this suboptimal bandgap choice resides in the convenient availability of highly optimized semiconducting organics and polymers having highest occupied molecular orbital and lowest unoccupied molecular orbital

(HOMO–LUMO) transitions in the visible region. Recent successes in colloidal nanoparticle PV in the visible and slightly into the NIR [9] derive similarly from the maturity of the CdS and CdSe materials systems, among the earliest and most perfected of colloidal nanoparticle materials systems [10].

The need for IR-bandgap solar cells becomes even more acute when one considers tandem and multijunction solar cells. As shown in Table I, higher overall solar power conversion efficiencies can be achieved when different-bandgap semiconductors are stacked atop one another. The first cell absorbs higher energy photons only, and provides a large open-circuit voltage; the next cells absorb the lower energy photons, and provide additive contributions to the open-circuit voltage. Assuming that each layer substantially absorbs its assigned spectral band, one can derive optimum bandgap choices for each member of the multijunction stack. If a rigorously series-connected multijunction architecture is employed, current matching throughout the stack adds the further constraint that the absorbed photon flux must match in each layer.

As seen in Table I, both layers in the tandem (two-junction) cell are in the IR, as indeed are all three layers of the optimum three-junction photovoltaic stacked device. Once again, the reason why most reports to date on solution-processed solar cells instead employ a pair of visible, or one visible and one NIR active layer, is based on practical availability of efficient solar cells in the visible region, and their absence in the NIR and especially the SWIR.

### B. Progress in Solution-Processed IR PV

We summarize progress on solution-processed IR PV in Table II. We use as proxy for performance the monochromatic power conversion efficiency. Our premise is that high-efficiency solar cells will require multiple junctions, so that in paving

TABLE II  
INFRARED PHOTOVOLTAIC POWER CONVERSION EFFICIENCIES  
AT THREE KEY BANDGAPS

	Date	PCE 1.5 $\mu\text{m}$	PCE 1 $\mu\text{m}$	PCE 700 nm	Type
[36]	Oct 2002			0.8% (k)	O
[13]	Jan 2005	.00004	.00008		QPM
[37]	May 2005			1.7*	O
[38]	Oct 2005		0.3		O
[39]	Nov 2005		0.001		QPM
[16]	Nov 2005		0.025		QPS
[40]	Apr 2006		0.8 *	2.7% *	O
[41]	Jan 2007			0.2% *	QPM
[17]	Apr 2007	0.8%	1.3%	1.4%	QD
[42]	Jul 2007		0.03%	0.7% *	O
[5]	Jul 2007			7.3% *	O
[43]	Oct 2007			0.8% *	O
[44]	Oct 2007		0.47 %	0.5% *	O
[43]	Oct 2007			~1% *	O
[12]	Jan 2008	3.8% *	4.2%	4.5%	QD
[14]	Jan 2008		3.7%	3.0%	QD

Key to Type column:

QPM: Quantum dots in a polymer matrix.

QPS: Pure quantum dots stacked atop a polymer.

QD: Pure quantum dots.

O: Pure organic (including small molecule, polymer, and C60 mixtures).

*Note.* In entries marked with a \* the monochromatic power conversion efficiency at the wavelength of interest was not reported explicitly in the cited work; however, external quantum efficiency (often in the form of a spectrum), open circuit voltage, and fill factor were provided, and thus, PCE was estimated via  $\text{PCE} = \text{EQE} \cdot (\text{qVoc}/\text{Ephoton}) \cdot \text{FF}$ .

the way toward high-efficiency cells, it makes sense to look at the performance of each junction that will ultimately become combined.

With this in mind we focus on three bandgaps—those corresponding to the three optimal choices for a three-junction multijunction PV device: 700 nm,  $\sim 1 \mu\text{m}$ , and  $> 1.5 \mu\text{m}$ .

Solar power conversion at a 700 nm bandgap has been accomplished with high efficiencies for more than two decades [11]. In the latest organic photovoltaic power conversion efficiency record, an AM1.5 efficiency of 6.5%, the lower bandgap layer in this tandem architecture provided 7.3% monochromatic power conversion efficiency at 700 nm [5].

It is the  $\sim 1 \mu\text{m}$  and  $> 1.5 \mu\text{m}$  performance levels that have, until recently, been almost unreported, owing to their very low level. Most striking has been progress in the vicinity of  $1 \mu\text{m}$ . While the target monochromatic power conversion efficiency needed to enable 10% AM1.5 power conversion efficiency in a three-junction cell is 13%, the latest experimentally reported values reach as high as 4.2% [12]. Performance in this spectral regime has progressed from well subpercent in the first report of January 2005 [13] to today's promising values. The realization of air-stable efficient IR devices represents a further recent accomplishment of note [14].

Also of interest is a marked trend in recent years in device architecture. First reports involved colloidal quantum dots embedded in a semiconducting polymer matrix [13], [15]. The premise of this approach was to create a charge-separating (type II) heterojunction to enable rapid dissociation of excitons into separated electrons and holes for independent transport to their respective contacts [16], [17]. Recent work [12] has instead employed a single phase of light-absorbing material—a colloidal quantum dot solid—in which excitons are created, and charges travel within the same phase to their respective contacts [18]. A Schottky barrier [19] was formed at the interface between a low-work-function metal contact (Al) and the p-type quan-

um dot solid. A depletion region of 150 nm resulted in which electrons and holes were induced to drift in opposite directions. The drift length in this quantum dot solid is considerably longer than 150 nm thanks to the modest mobilities ( $2 \times 10^{-4}$  to  $1 \times 10^{-3} \text{ cm}^2/\text{V}\cdot\text{s}$ ) of each carrier and the long lifetimes resulting from  $\sim 40\text{-}\mu\text{s}$ -lifetime trap states at the nanoparticle surfaces. A considerable further contribution to the current flowing in these devices arose from the diffusion of carriers generated outside of the depletion region toward the depletion region for separation and ensuing extraction.

### III. OPTICAL SENSORS

The realization of highly sensitive IR photodetectors, suited to image sensor technology, and fabricated using simple solution-processing, is the area that has seen the greatest strides in performance in recent years. Already, after only two years' worth of optimization, solution-processed photodetectors are now as sensitive as the highest-performance epitaxial crystal devices.

#### A. Requirements for High-Performance Solution-Processed Photodetectors

External quantum efficiency (EQE), the ratio of photocarriers collected to photons incident, is a familiar figure of merit relevant to the sensitivity of a photodiode; however, EQE conveys only the signal, but not the noise component, of the signal-to-noise considerations essential to quantifying sensitivity.

Noise-equivalent power (NEP) quantifies the optical power incident on a photodiode at which  $\text{SNR} = 1$ . Since this figure depends on area, it does not allow comparison among devices of vastly different areas.

Comparing across a wide range of detector areas is possible only in the context of a model predicting areal scaling of NEP. The use of normalized detectivity  $D^*$ , equal to the square root of the area $\times$ bandwidth product of a device divided by NEP, provides normalization with respect to bandwidth and area. Physically, the square-root dependence is justified if the noise is dominated either by dark current shot noise or by Johnson noise. Because one of these sources does often dominate noise,  $D^*$  is a useful figure of merit and is widely used, especially in the IR community, to compare devices having different areas.

#### B. Progress in Solution-Processed Photodetectors

We present in Table III the progress in time of solution-processed photodetector performance.

In 2000, Bulovic *et al.* reported a very-high-quantum-efficiency photodiode ( $\text{EQE} = 75\%$ ) operating in the visible region [20]. The device was based on a very thin organized absorbing layer that captured the bulk of light spanning the visible region using a material thickness of only hundreds of angstroms. This device also exhibited what was, for a solution-processed device relying on electronic transport, a remarkable 3 dB bandwidth in the many hundreds of megahertz. The sensitivity of this device was not reported.

In a 2005 report, Bulovic *et al.* demonstrated another vertical photodiode [21] that incorporated quantum dots, a

TABLE III  
INFRARED (IR) PHOTODETECTOR SENSITIVITIES AND BANDWIDTHS

Ref	Date	EQE	Lambda	BW	D* (cm Hz <sup>1/2</sup> W <sup>-1</sup> )
[20]	Jun 2000	75% at 10 V bias	450-750 nm	430 MHz	
[21]	Nov 2005	15-24% at 5 V 0.08-0.23% unbiased	350-575 nm	50 kHz	> 10 <sup>2</sup> <sup>(a)</sup>
[45]	Jul 2007	0.01% <sup>(b)</sup>	Visible		
[34]	Jan 2008	20% in SWIR unbiased 40% in Visible unbiased	400 – 1600 nm	60 kHz	1x10 <sup>12</sup>

<sup>(a)</sup> Based on reported 3-sigma detection intensity limit of 10 W/cm<sup>2</sup> for device area 0.01 cm<sup>2</sup> and measurement bandwidth 1 MHz.

<sup>(b)</sup> Estimated based on reported responsivity of 6x10<sup>-5</sup> A/W.

(a)

Ref	Date	Responsivity	Lambda	BW	D*
[22]	Jul 2006	> 1000 A/W	400 – 1400 nm	20 Hz	2x10 <sup>13</sup>
[23]	Sep 2007	> 100 A/W	400 – 800 nm	20 Hz	5x10 <sup>12</sup>

(b)

strategy compatible with extension of photodiode sensitivities into new spectral regimes using quantum-size-effect tuning. These devices exhibited an absorbance and external quantum efficiency that were both influenced by the dots' spectrum. Under a significant bias, the devices exhibited high external quantum efficiencies ranging from 17% to 24%. Again, no sensitivity was reported, and high EQEs were obtained only when bias was such as to result in appreciable dark currents.

In 2006, Konstantatos *et al.* reported [22] a device that instead employed a photoconductive mechanism. Fabrication was very simple: a layer of quantum dots was spin-coated onto a pair of preexisting parallel gold electrodes. Current flowed laterally under bias in this device. The device exhibited very considerable photoconductive gain, well into the thousands under high (50 V) bias, and more practically, gains in the ten-to-hundred range under few-volts biases. Considerable effort was made to minimize the noise current through optimization of the various chemical treatments on the colloidal quantum dots and the films made therefrom. The record value of  $2 \times 10^{13}$  Jones D\* was achieved by optimizing materials processing conditions to produce a noise current that came within 3 dB of the available physical limit.

The reported sensitivities are superior to the best values obtained from InGaAs photodiodes operating in the same wavelength range and at the same temperature. The use of a large photoconductive gain provides the added advantage of simplifying the readout circuit design by embedding gain within the sensor material even before the analog readout circuit.

Konstantatos *et al.* reported [23] in 2007 that the analogous strategy, extrapolated to the visible region, could successfully be implemented. Here, the authors similarly obtained large gains and comparable D\* values. They did so using the same materials system as in [22] by tuning the synthesis parameters so as to reduce the quantum dot diameter, thereby shortening the cutoff wavelength of absorbance via quantum-size-effect tuning.

Taken together, these works on pure-colloidal quantum-dot photoconductive photodetectors suggest the possibility of realizing highly sensitive multispectral imaging systems using straightforward tuning within a single materials system.

The two photoconductive photodetector reports also reveal one of the challenges in this approach. Long-lived trap states [24], crucial to achieving high gain, reduce the frequency of response of the materials. These devices operated with 3 dB bandwidths are suitable for imaging, but not for higher bandwidth applications.

Fortunately, a solution has recently been found to the lag problem: it was recently shown [25] that states possessing a substantially single-valued time constant can be introduced into a photoconductive material, imparting a simultaneous combination of attractive gain and video-frame-rate-compatible response.

#### IV. OPTICAL SOURCES

Here, we focus on IR optical sources; there already exists a vast and well-summarized [26] literature on visible light emitters

of great interest in displays and lighting, including systems achieving low cost and/or physical flexibility.

Colloidal quantum-dot-based electroluminescent devices operating in the IR were first reported in the early 2000s [27], [28]. These devices exhibited internal quantum efficiencies of about 1% and a maximum external quantum efficiency of about 0.5% [27]. Subsequent studies sought to investigate systematically at a means of increasing efficiency. One report [29] purposed to increase the photoluminescence quantum efficiency of the light-emitting species, achieving over 50% quantum yield in solution and 12% quantum yield in thin solid films. Optimization of injection conditions [30] led to an internal quantum efficiency to approximately 2%.

Of great interest, especially in communications, is a coherent, directional source with narrow spectral linewidth: a laser. There exists one report of SWIR lasing in colloidal quantum dot films [31]. Optically pumped lasing was obtained at 1.54  $\mu\text{m}$  wavelength. The method of fabrication was very simple: a glass capillary was dipped into a suspension of colloidal quantum dots and dried to produce a smooth, low-scattering film inside the capillary. A whispering gallery mode laser having a well-defined threshold in emitted optical power as a function of pump power was demonstrated. As anticipated, in this zero-dimensional system, a very low temperature sensitivity to the lasing wavelength—ten times lower than in traditional semiconductor quantum wells—was obtained.

We also summarize in this section the progress on optical modulators operating in the SWIR regime. Such devices offer the potential to add an information-bearing signal atop an existing optical carrier. In 2005, the first study of IR colloidal quantum dot modulators [32] reported modulators across the entire band, 1200–1700 nm, thus more than addressing the spectral range of interest in coarse wavelength-division multiplexed fiber-optical communications. This first report, however, described low modulation depths (upto 10  $\text{cm}^{-1}$ ) and relatively narrow modulation bandwidths (hundreds of hertz).

A recent report [33] details a simple solution-processed IR optical modulator that combines straightforward solution-processing, modulation at 1.55  $\mu\text{m}$  of particular interest in communications, 30% modulation depth, and 120 kHz modulation bandwidth with significant modulation depth out to 1 MHz.

## V. SYNOPSIS AND PROSPECTS

One broad conclusion can be drawn from the solution-processed optoelectronics literature of the past few years: preconceived notions as to the limitations of these materials may be ill-founded.

Certainly—as one would expect in any materials system engineered for high performance only within the past few years—challenges remain. In PV, efficiencies are starting to approach, but have yet to cross, the 10% threshold widely viewed as important to widespread commercial impact. In light emission, broadband IR efficiencies require further progress before reaching commercial viability, and lasing has yet to be demonstrated with a combination of room-temperature operation and electrically driven excitation. In all areas of application, crucially important

engineering challenges—stabilization of materials via encapsulation, mass production, and successful integration onto large substrates—remain to be tackled and successfully addressed.

Striking though is the set of assumptions about solution-processed optoelectronics that have been invalidated through recent findings.

- 1) In light of the highly desirable ease of processing and integration of colloidal quantum dots with a wide range of substrates, one might have assumed that performance might have to be traded off in favor of low cost and convenience; however, record  $D^*$  photodetectors [22] and high power conversion efficiency PV [12], [14] experimentally contradict any such assumptions.
- 2) One might still assume that while low cost, large area, integrability, and sensitivity or efficiency could be combined, perhaps speed of response could not; however, tens of kilohertz and even megahertz speeds of response from sensors [34] and modulators [33] experimentally contradict any such assumptions.
- 3) One might assume that a new materials system optimized to open up a new spectral regime—especially the SWIR—might automatically be relegated to niche applications; however, high-visible-wavelength efficiencies [12], [14] and sensitivities [23] from these same devices contradict experimentally any such assumptions.

## REFERENCES

- [1] M. A. Green, K. Emery, Y. Hisikawa, and W. Warta, "Solar cell efficiency tables (version 30)," *Progr. Photovoltaics: Res. Appl.*, vol. 15, pp. 425–430, 2007.
- [2] Z. Cheng, M. T. Currie, C. W. Leitz, G. Taraschi, E. A. Fitzgerald, J. L. Hoyt, and D. A. Antoniadis, "Electron mobility enhancement in strained-Si n-Mosfets fabricated on SiGe-on-insulator (SGOI) substrates," *IEEE Electron Device Lett.*, vol. 22, no. 7, pp. 321–323, Jul. 2001.
- [3] A. Liu, R. Jones, L. Liao, D. Samara-Rubio, D. Rubin, O. Cohen, R. Nicolaescu, and M. Paniccia, "A high speed silicon optical modulator based on a metal oxide semiconductor capacitor," *Nature*, vol. 427, pp. 615–618, 2004.
- [4] E. R. Fossum, "CMOS image sensors: Electronic camera-on-a-chip," *IEEE Trans. Electron Devices*, vol. 44, no. 10, pp. 1689–1698, Oct. 1997.
- [5] Y. K. Jin, K. Lee, N. E. Coates, D. Moses, T.-Q. Nguyen, M. Dante, and A. J. Heeger, "Efficient tandem polymer solar cells fabricated by all-solution processing," *Science*, vol. 317, pp. 222–225, 2007.
- [6] S. Coe, W. Woo, M. Bawendi, and V. Bulović, "Electroluminescence from single monolayers of nanocrystals in molecular organic devices," *Nature*, vol. 420, pp. 800–803, 2002.
- [7] M. Ettenberg, "A little night vision," *Adv. Imag.*, vol. 20, pp. 29–32, 2005.
- [8] B. E. Lemoff, "Coarse WDM transceivers," *Opt. Photon. News*, vol. 13, pp. S8–S14, 2002.
- [9] I. Gur, N. A. Fromer, M. L. Geier, and A. P. Alivisatos, "Materials science: Air-stable all-inorganic nanocrystal solar cells processed from solution," *Science*, vol. 310, pp. 462–465, 2005.
- [10] C. B. Murray, D. J. Norris, and M. G. Bawendi, "Synthesis and characterization of nearly monodisperse CdE (E = S, Se, Te) semiconductor nanocrystallites," *J. Amer. Chem. Soc.*, vol. 115, pp. 8706–8715, 1993.
- [11] C. W. Tang, "Two-layer organic photovoltaic cell," *Appl. Phys. Lett.*, vol. 48, pp. 183–185, 1986.
- [12] K. W. Johnston, A. G. Pattantyus-Abraham, J. P. Clifford, S. H. Myrskog, D. D. MacNeil, L. Levina, and E. H. Sargent, "Schottky-quantum dot photovoltaics for efficient infrared power conversion," *Appl. Phys. Lett.*, vol. 92, pp. 151115-1–151115-3, 2008.
- [13] S. A. McDonald, G. Konstantatos, S. Zhang, P. W. Cyr, E. J. D. Klem, L. Levina, and E. H. Sargent, "Solution-processed PbS quantum dot infrared photodetectors and photovoltaics," *Nature Mater.*, vol. 4, pp. 138–142, 2005.

- [14] G. Koleilat, L. Levina, H. Shukla, S. Myrskog, S. Hinds, A. Pattantyus-Abraham, and E. H. Sargent, "Efficient, stable infrared photovoltaics based on solution-cast colloidal quantum dots," *ACS Nano*, vol. 2, pp. 1–8, 2008.
- [15] S. A. McDonald, P. W. Cyr, L. Levina, and E. H. Sargent, "Photoconductivity from PbS-nanocrystal/semiconducting polymer composites for solution-processible, quantum-size tunable infrared photodetectors," *Appl. Phys. Lett.*, vol. 85, pp. 2089–2091, 2004.
- [16] A. Maria, P. W. Cyr, E. J. D. Klem, L. Levina, and E. H. Sargent, "Solution-processed infrared photovoltaic devices with >10% monochromatic internal quantum efficiency," *Appl. Phys. Lett.*, vol. 87, pp. 1–3, 2005.
- [17] E. J. D. Klem, D. D. MacNeil, P. W. Cyr, L. Levina, and E. H. Sargent, "Efficient solution-processed infrared photovoltaic cells: Planarized all inorganic bulk heterojunction devices via inter-quantum-dot bridging during growth from solution," *Appl. Phys. Lett.*, vol. 90, pp. 183113-1–183113-3, 2007.
- [18] K. W. Johnston, A. G. Pattantyus-Abraham, J. P. Clifford, S. H. Myrskog, S. Hoogland, H. Shukla, E. J. D. Klem, L. Levina, and E. H. Sargent, "Efficient Schottky-quantum-dot photovoltaics: The roles of depletion, drift, and diffusion," *Appl. Phys. Lett.*, vol. 92, pp. 122111-1–122111-3, 2008.
- [19] J. P. Clifford, K. W. Johnston, L. Levina, and E. H. Sargent, "Schottky barriers to colloidal quantum dot films," *Appl. Phys. Lett.*, vol. 91, pp. 253117-1–253117-3, 2007.
- [20] P. Peumans, V. Bulović, and S. R. Forrest, "Efficient, high-bandwidth organic multilayer photodetectors," *Appl. Phys. Lett.*, vol. 76, pp. 3855–3857, 2000.
- [21] D. C. Oertel, M. G. Bawendi, A. C. Arango, and V. Bulović, "Photodetectors based on treated CdSe quantum-dot films," *Appl. Phys. Lett.*, vol. 87, pp. 1–3, 2005.
- [22] G. Konstantatos, I. Howard, A. Fischer, S. Hoogland, J. Clifford, E. Klem, L. Levina, and E. H. Sargent, "Ultrasensitive solution-cast quantum dot photodetectors," *Nature*, vol. 442, pp. 180–183, 2006.
- [23] G. Konstantatos, J. Clifford, L. Levina, and E. H. Sargent, "Sensitive solution-processed visible-wavelength photodetectors," *Nature Photon.*, vol. 1, pp. 531–534, 2007.
- [24] G. Konstantatos and E. H. Sargent, "PbS colloidal quantum dot photoconductive photodetectors: Transport, traps, and gain," *Appl. Phys. Lett.*, vol. 91, pp. 173505-1–173505-3, 2007.
- [25] G. Konstantatos, L. Levina, A. Fischer, and E. H. Sargent, "Engineering the temporal response of photoconductive photodetectors via selective introduction of surface trap states," *Nano Lett.*, vol. 8, pp. 1446–1450, Apr. 2008.
- [26] R. H. Friend, R. W. Gymer, A. B. Holmes, J. H. Burroughes, R. N. Marks, C. Taliani, D. D. C. Bradley, D. A. Dos Santos, J. L. Brédas, M. Logdlund, and W. R. Salaneck, "Electroluminescence in conjugated polymers," *Nature*, vol. 397, pp. 121–128, 1999.
- [27] N. Tessler, V. Medvedev, M. Kazes, S. Kan, and U. Banin, "Efficient near-infrared polymer nanocrystal light-emitting diodes," *Science*, vol. 295, pp. 1506–1508, 2002.
- [28] L. Bakueva, S. Musikhin, M. A. Hines, T.-F. Chang, M. Tzolov, G. D. Scholes, and E. H. Sargent, "Size-tunable infrared (1000–1600 nm) electroluminescence from PbS quantum-dot nanocrystals in a semiconducting polymer," *Appl. Phys. Lett.*, vol. 82, pp. 2895–2897, 2003.
- [29] T.-F. Chang, A. Maria, P. W. C. V. Sukhovatkin, L. Levina, and E. H. Sargent, "Ten-fold improvement in the photoluminescence quantum efficiency of quantum-size-effect-tunable (1000–2000 nm) and solution-processed PbS nanocrystal films," in *Proc. 2005 Lasers Electro-Opt. (CLEO) Conf.*, pp. 618–620.
- [30] G. Konstantatos, C. Huang, L. Levina, Z. Lu, and E. H. Sargent, "Efficient infrared electroluminescent devices using solution-processed colloidal quantum dots," *Adv. Funct. Mater.*, vol. 15, pp. 1865–1869, 2005.
- [31] S. Hoogland, V. Sukhovatkin, H. Shukla, J. P. Clifford, L. Levina, and E. H. Sargent, "Megahertz-frequency solution-processed infrared optical modulators based on colloidal quantum dots," *Opt. Exp.*, vol. 16, no. 9, pp. 6683–6691, 2008.
- [32] E. J. D. Klem, L. Levina, and E. H. Sargent, "PbS quantum dot electroabsorption modulation across the extended communications band 1200–1700 nm," *Appl. Phys. Lett.*, vol. 87, pp. 053101–053101-3, 2005.
- [33] S. Hoogland, V. Sukhovatkin, H. Shukla, J. P. Clifford, L. Levina, and E. H. Sargent, "Megahertz-frequency solution-processed infrared optical modulators based on colloidal quantum dots," *Opt. Exp.*, vol. 16, no. 9, pp. 6683–6691, 2008.
- [34] J. P. Clifford and E. H. Sargent, "Fast, sensitive, spectrally-tunable solution-processed photodetectors," submitted for publication.
- [35] A. Martí and G. L. Araújo, "Limiting efficiencies for photovoltaic energy conversion in multigap systems," *Sol. Energy Mater. Sol. Cells*, vol. 43, pp. 203–222, 1996.
- [36] C. J. Brabec, C. Winder, N. S. Sariciftci, J. C. Hummelen, A. Dhanabalan, P. A. Van Hal, and R. A. J. Janssen, "A low-bandgap semiconducting polymer for photovoltaic devices and infrared emitting diodes," *Adv. Funct. Mater.*, vol. 12, pp. 709–712, 2002.
- [37] F. Zhang, E. Perzon, X. Wang, W. Mammo, M. R. Andersson, and O. Inganäs, "Polymer solar cells based on a low-bandgap fluorene copolymer and a fullerene derivative with photocurrent extended to 850 nm," *Adv. Funct. Mater.*, vol. 15, pp. 745–750, 2005.
- [38] X. Wang, E. Perzon, F. Oswald, F. Langa, S. Admassie, M. R. Andersson, and O. Inganäs, "Enhanced photocurrent spectral response in low-bandgap polyfluorene and C70—derivative-based solar cells," *Adv. Funct. Mater.*, vol. 15, pp. 1665–1670, 2005.
- [39] S. Zhang, P. W. Cyr, S. A. McDonald, G. Konstantatos, and E. H. Sargent, "Enhanced infrared photovoltaic efficiency in PbS nanocrystal/semiconducting polymer composites: 600-fold increase in maximum power output via control of the ligand barrier," *Appl. Phys. Lett.*, vol. 87, pp. 1–3, 2005.
- [40] M. M. Wienk, M. G. R. Turbiez, M. P. Struijk, M. Fonrodona, and R. A. J. Janssen, "Low-band gap poly(di-2-thienylthienopyrazine): Fullerene solar cells," *Appl. Phys. Lett.*, vol. 88, pp. 15351-1–15351-3, 2006.
- [41] S. Guenes, K. P. Fritz, H. Neugebauer, N. S. Sariciftci, S. Kumar, and G. D. Scholes, "Hybrid solar cells using PbS nanoparticles," *Sol. Energy Mater. Sol. Cells*, vol. 91, pp. 420–423, 2007.
- [42] M. Sun, L. Wang, X. Zhu, B. Du, R. Liu, W. Yang, and Y. Cao, "Near-infrared response photovoltaic device based on novel narrow band gap small molecule and PCBM fabricated by solution processing," *Sol. Energy Mater. Sol. Cells*, vol. 91, pp. 1681–1687, 2007.
- [43] E. Bundgaard, S. E. Shaheen, F. C. Krebs, and D. S. Ginley, "Bulk heterojunctions based on a low band gap copolymer of thiophene and benzothiadiazole," *Sol. Energy Mater. Sol. Cells*, vol. 91, pp. 1631–1637, 2007.
- [44] E. Perzon, F. Zhang, M. Andersson, W. Mammo, O. Inganäs, and M. R. Andersson, "A conjugated polymer for near infrared optoelectronic applications," *Adv. Mater.*, vol. 19, pp. 3308–3311, 2007.
- [45] I. Nausieda, K. Ryu, I. Kymissis, A. I. Akinwande, V. Bulovic, and C. G. Sodini, "An organic imager for flexible large area electronics," in *Proc. IEEE Int. Solid-State Circuits Conf.* San Francisco, CA, Feb. 2007, pp. 72–73.



**Edward (Ted) H. Sargent** (S'97–M'98–SM'03) received the B.Sc. degree in engineering physics from Queen's University, Kingston, ON, Canada, in 1995, and the Ph.D. degree in electrical engineering from the University of Toronto, Toronto, ON, in 1998.

In 1998, he joined the faculty of the University of Toronto, where he is currently a Professor and the Canada Research Chair in Nanotechnology. He is the author of the book *The Dance of Molecules: How Nanotechnology is Changing Our Lives*, which was published in the USA and Canada in 2006 and has since been reprinted in Korean, French, and Spanish.

Prof. Sargent was named as one of the world's top innovators in 2003 in *MIT's Technology Review Magazine*. In 2005, *Scientific American* named him to their annual list of 50 outstanding leaders in science and technology for advancing the field of solar energy by developing paintable solar cells that capture the infrared half of the sun's power reaching the earth. In 2008, he was named a King Abdullah University of Science and Technology (KAUST) Investigator to help advance his research on low-cost large-area solar cells.